DOI: 10.63527/1607-8829-2023-1-33-43

V. A. Romaka *doc. tech. science, professor*[1],
Yu. V. Stadnyk *cand. chem. science*[2],
L. P. Romaka *cand. chem. science*[2],
P. Yu. Demchenko [2],
A. M. Horyn *cand. chem. science*[2],
T. I. Lukovskyi [1]

[1]National University "Lvivska Politechnika", 12,
S. Bandera Str., Lviv, 79013, Ukraine, *e-mail: vromaka@polynet.lviv.ua*
[2]Ivan Franko National University of Lviv, 6, Kyryla and Mefodiya Str.,
Lviv, 79005, Ukraine, *e-mail: lyubov.romaka@lnu.edu.ua*

EXPERIMENTAL INVESTIGATIONS OF THE PROPERTIES OF A NEW THERMOELECTRIC MATERIAL $Tm_{1-x}V_xNiSb$

The structural, kinetic, and energy properties of the $Tm_{1-x}V_xNiSb$ thermoelectric material were studied in the ranges: T=80–400 K, x=0–0.10. It is shown that V atoms can simultaneously occupy different crystallographic positions in different ratios, generating defects of acceptor and donor nature. This gives rise to the corresponding acceptor and donor states in the bandgap ε_g $Tm_{1-x}V_xNiSb$. The mechanism of formation in $Tm_{1-x}V_xNiSb$ of two types of acceptor states with different depth of occurrence was established: shallow acceptors generated by vacancies in the structure of half-Heusler phase TmNiSb, and deep acceptors formed by defects when Ni atoms are replaced by V in the 4c position. The ratio of the concentrations of generated defects determines the position of the Fermi level ε_F and the conduction mechanisms. The investigated $Tm_{1-x}V_xNiSb$ solid solution is a promising thermoelectric material. Bibl. 12, Fig. 7.

Keywords: electronic structure, electric resistivity, Seebeck coefficient.

Introducion

Semiconductor solid solutions based on half-Heusler phases *RNiSb* (*R* – rare earth metals of the Ittrium subgroup) is a new and promising class of thermoelectric materials with a high efficiency of thermal into electric energy conversion [1]. The formation of substitutional solid solutions based on *RNiSb* is accompanied by the generation of defects of donor or acceptor nature in the crystal structure, and corresponding energy states appear in the bandgap ε_g. This makes it possible to smoothly change the values of electrical conductivity $\sigma(T)$, Seebeck coefficient $\alpha(T)$ and thermal conductivity $\kappa(T)$, and the process of optimizing the properties of thermoelectric material becomes predictable [2].

In this context, it seems interesting to study a new thermoelectric material $Tm_{1-x}V_xNiSb$, when *V* ($3d^34s^2$) atoms are introduced into the structure of the half-Heusler phase *TmNiSb* (structure type *MgAgAs*, spatial group $F\bar{4}3m$ [3]) by substituting in the crystallographic position 4*a* of atoms *Tm* ($5d^06s^2$). The introduction of *V* atoms into the structure of the *TmNiSb* compound should generate defects of donor nature (*V* has more *d*-electrons than *Tm*), and corresponding donor states will appear in the bandgap ε_g of $Tm_{1-x}V_xNiSb$. The *TmNiSb* compound was discovered during the study of phase equilibria in the *Tm-Ni-Sb* system which turned out to be a hole-type semiconductor, as indicated by the positive values of the Seebeck coefficient α (Fig. 1*a*) [4, 5].

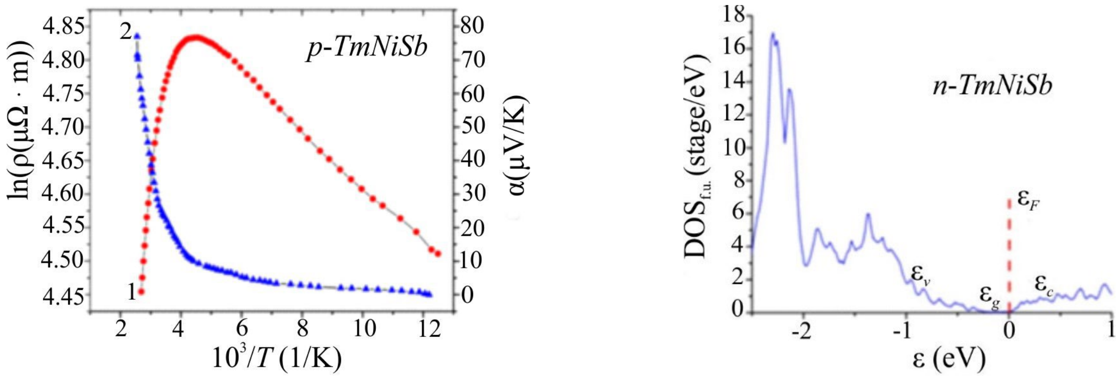

a) *b)*

Fig. 1. Temperature dependences of electrical resistivity ρ (1) and the Seebeck coefficient α (2) (a) and distribution of the density of electronic states DOS (b) of the basic semiconductor TmNiSb [5]

At the same time, simulation of the electronic structure for the ordered version of the *TmNiSb* crystal structure showed that the Fermi level ε_F lies near the edge of the conduction band ε_C (Fig. 1 *b*), and electrons are the majority carriers. The inconsistency of the experimental and simulation results prompts us to establish the crystal and electronic structure of the *p-TmNiSb* basic semiconductor as close as possible to the real state. In addition, since the atomic radius of *V* (r_V = 0.134 nm) is smaller than *Tm* (r_{Tm} = 0.174 nm) and close to the atomic radius of *Ni* (r_{Ni} = 0.125 nm), the formation of a $Tm_{1-x}V_xNiSb$ substitutional solid solution may be accompanied by unpredictable changes in the crystal and electronic structure. This is precisely the subject of the following study. After all, knowledge of the peculiarities of the dynamics of the crystal and electronic structures of the $Tm_{1-x}V_xNiSb$ semiconductor allows the appropriate doping to generate energy states that will meet the conditions for obtaining the maximum values of the thermoelectric figure of merit *Z* [2], and the process of optimizing properties will be predictable.

Previous studies of the related semiconductor thermoelectric materials based on half-Heusler phases, in particular, $Lu_{1-x}V_xNiSb$ [6], $Lu_{1-x}Zr_xNiSb$ [7] and $Lu_{1-x}Sc_xNiSb$ [8], allowed establishing the disorder and defectiveness of the crystal structure of the basic semiconductor *p-LuNiSb.* It was shown that there are vacancies (V_{ac}) in positions 4*a* of *Lu* atoms and 4*c* of *Ni* atoms (Fig. 2), which generate structural defects of acceptor nature and corresponding acceptor states in the bandgap ε_g of the *p-LuNiSb* semiconductor. The presence of vacancies in the structure of the *LuNiSb* compound fundamentally changes the mechanism of entry of impurity atoms into its crystal structure when optimizing the properties of the thermoelectric material to obtain the maximum values of the thermoelectric figure of merit *Z* ($Z(T)=\alpha^2(T)/\sigma(T)\cdot\kappa(T)$) [2].

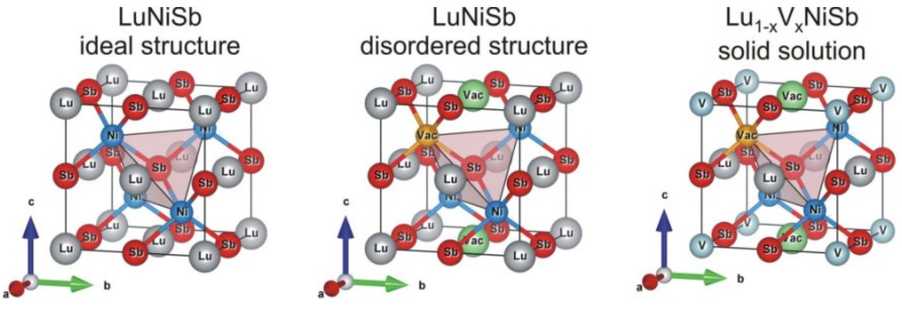

Fig. 2. Models of variants of the crystal structure LuNiSb and $Lu_{1-x}V_xNiSb$

Thus, doping *p-LuNiSb* by atoms with large atomic radii, in particular, *Zr* (r_{Zr} = 0.160 nm) and *Sc* (r_{Sc} = 0.164 nm), by substituting in position 4*a* the rare earth metal atom *Lu* (r_{Lu} = 0.173 nm) did not lead to occupation by doping atoms of other crystallographic positions. Moreover, the substitution of *Lu* ($5d^16s^2$) by *Sc* ($3d^14s^2$) generated in $Lu_{1-x}Sc_xNiSb$ defects of neutral nature (*Lu* and *Sc* are located in the same group of the periodic system of chemical elements)), and in the case of introducing *Zr* ($4d^25s^2$) atoms– defects of donor nature (*Zr* has more *d*-electrons). Simulation of the free energy $\Delta G(x)$ (Helmholtz potential) and mixing enthalpy ΔH_{mix} showed the energetic feasibility of the existence of $Lu_{1-x}Zr_xNiSb$ and $Lu_{1-x}Sc_xNiSb$ solid solutions [7, 8].

When doping *p-LuNiSb* with *V* ($3d^34s^2$) atoms, introduced into the structure by substitution in position 4*a* of *Lu* atoms, *V* atoms simultaneously occupied different crystallographic positions in different ratios [6]. The prerequisite for such changes in the crystal and electronic structures of $Lu_{1-x}V_xNiSb$ was the proximity of the atomic radii of *V* (r_V = 0.134 nm) and *Ni* (r_{Ni} = 0.125 nm), when defects of acceptor and donor nature are generated, and in the bandgap ε_g the respective energy states appear.

The results of the study of the structural, kinetic, and energy properties of the semiconductor solid solution $Tm_{1-x}V_xNiSb$, $x = 0 - 0.10$, presented below will allow us to understand the nature of the defects of the basic semiconductor *p-TmNiSb*, which will make the process of optimizing the characteristics of the thermoelectric material predictable.

Research methods

The crystal structure, electrokinetic and energy properties of the $Tm_{1-x}V_xNiSb$, $x = 0 - 0.1$ solid solution were studied. $Tm_{1-x}V_xNiSb$ samples were synthesized by fusing a batch of initial components in an electric arc furnace in an inert argon atmosphere followed by homogenizing annealing for 720 h at a temperature of 1073 K. Arrays of diffraction data were obtained using a STOE STADI P powder diffractometer ($CuK\alpha_1$ radiation). Crystallographic parameters were calculated using the Fullprof program [9]. The chemical and phase compositions of the samples were monitored by a microprobe analyzer (EPMA, energy-dispersive *X*-ray analyzer). We measured the temperature and concentration dependences of the resistivity (ρ) and the Seebeck coefficient (α) relative to the copper of $Tm_{1-x}V_xNiSb$, $x = 0 - 0.10$ samples, in the temperature range $T = 80 - 400$ KW.

Research on the structural properties of $Tm_{1-x}V_xNiSb$

X-ray phase and structural analyses of $Tm_{1-x}V_xNiSb$, $x = 0 - 0.1$ samples showed that the diffractograms of the samples contain no traces of other phases and are indexed in the *MgAgAs* structural type. X-ray structural studies also made it possible to establish the nature of change in the unit cell period $a(x)$ of $Tm_{1-x}V_xNiSb$. Based on the fact that the atomic radius of *Tm* (r_{Tm} = 0.174 nm) is much larger than the atomic radius of *V* (r_V = 0.134 nm), we expected to obtain a decrease in the values of the unit cell period $a(x)$ when *Tm* atoms are replaced by *V* atoms in the position 4*a*. Such substitution should have generated in the crystal structure of $Tm_{1-x}V_xNiSb$ defects of donor nature and their corresponding impurity donor states in the bandgap ε_g of the semiconductor.

However, the results of *X*-ray structural analysis of $Tm_{1-x}V_xNiSb$ solid solution samples do not show, as expected, a monotonous decrease in the values of the unit cell period $\alpha(x)$ (Fig. 3). Thus, in the area of concentrations $x = 0 - 0.03$, the values of the period $\alpha(x)$ increase, pass through a maximum, and begin to decrease at $x > 0.03$. The non-monotonic change in the values of the fundamental structural parameter of the $Tm_{1-x}V_xNiSb$ solid solution is experimental evidence that *V* atoms introduced into the *TmNiSb* compound not only replace *Tm* atoms in position 4*a*, but also partially occupy other crystallographic positions. By the way, when studying the related semiconductor solid solution $Lu_{1-x}V_xNiSb$, we obtained a similar behavior of the unit cell period α(*x*) (Fig. 3, inset) [6]. Studies have shown that in $Lu_{1-x}V_xNiSb$, *V* atoms simultaneously occupy the crystallographic positions 4*a* of *Lu* atoms and 4*c* of *Ni* atoms in different ratios, generating structural defects of acceptor and donor nature.

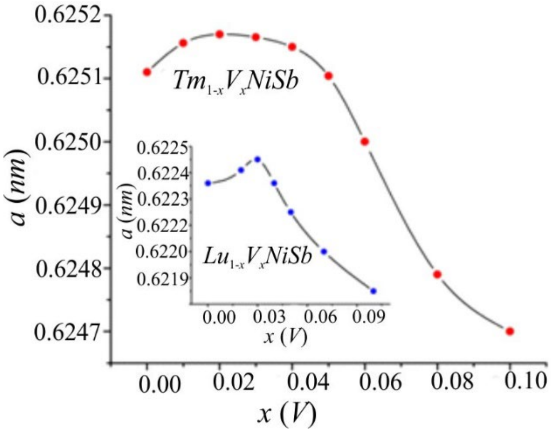

Fig. 3. Change in the values of the unit cell period a(x) of $Tm_{1-x}V_xNiSb$; inset: change in the unit cell period a(x) of $Lu_{1-x}V_xNiSb$ [6]

Based on geometric considerations, we can assume that the increase in the unit cell period *a*(*x*) in the area of concentrations $x = 0 - 0.03$ $Tm_{1-x}V_xNiSb$ could simultaneously be caused by two processes:

a) occupation by *V* atoms of vacancies (V_{ac}) in the crystallographic position 4*a*;

b) partial occupation by *V* atoms of the 4*c* position of *Ni* atoms, since the atomic radius *V* (r_V = 0.134 nm) is greater than the atomic radius of *Ni* (r_{Ni} = 0.125 nm).

In this case, the following processes will occur in the electronic structure of the $Tm_{1-x}V_xNiSb$ solid solution at concentrations of $x = 0 - 0.03$:

a) occupation by *V* atoms of vacancies (V_{ac}) in position 4*a*, which acted as structural defects of the acceptor nature and generated acceptor states, will lead to the simultaneous elimination of defects of acceptor nature and now generates effects of donor nature with the appearance in the bandgap ε_g of the corresponding donor states;

b) occupation by *V* atoms of the 4*c* position of *Ni* atoms generates structural defects of acceptor nature, since *V* ($3d^34s^2$) atom has fewer *d*-electrons than *Ni* ($3d^84s^2$) atom, and corresponding acceptor states are generated in the bandgap.

A decrease in the unit cell period *a*(*x*) in the semiconductor solid solution $Tm_{1-x}V_xNiSb$ at concentrations $x > 0.03$ can only cause the replacement of *Tm* atoms (r_{Tm} = 0.174 nm) by *V* atoms (r_V = 0.134 nm) in the crystallographic position 4*a*. In this case, structural defects of donor nature will be generated in the $Tm_{1-x}V_xNiSb$ semiconductor, since *V* ($3d^34s^2$) atoms have more *d*-electrons than *Tm* ($5d^06s^2$) atoms, and corresponding donor states will appear in the bandgap.

Insignificant concentrations of impurity *V* atoms and relatively low accuracy of *X*-ray structural studies did not allow establishing the fact of ordering the crystal structure of the semiconductor. Therefore, we are aware that the results of structural studies do not fully reflect possible transformations in the structure of $Tm_{1-x}V_xNiSb$. Therefore, the above considerations regarding changes in the crystal structure based on the behavior of the unit cell period *a*(*x*) of $Tm_{1-x}V_xNiSb$ are of an evaluative nature. The following results of studying the kinetic and energy properties of $Tm_{1-x}V_xNiSb$ will make it possible to clarify conclusions about possible changes in the structure of the thermoelectric material. On this basis, it will be possible in the future to model crystal and electronic structures as close as possible to the real state of matter, which will be the basis for optimizing the kinetic properties of the thermoelectric material by choosing doping conditions.

Research on the electrokinetic and energy properties of $Tm_{1-x}V_xNiSb$

The temperature and concentration dependences of the resistivity ρ and the Seebeck coefficient α for the samples $Tm_{1-x}V_xNiSb$, $x = 0.02 - 0.10$, are given in Figs. 4 - 6. The dependences $\ln(\rho(1/T))$ and $\alpha(1/T)$ for $Tm_{1-x}V_xNiSb$, $x = 0 - 0.10$ are typical for doped and compensated semiconductors with high- and low-temperature activation regions, which indicates the presence of several mechanisms of electrical conductivity. The dependences $\ln(\rho(1/T))$ for $Tm_{1-x}V_xNiSb$, $x = 0 - 0.10$ samples are described using a well-known relation (1) [10, 11]:

$$\rho^{-1}(T) = \rho_1^{-1}\exp\left(-\frac{\varepsilon_1^{\rho}}{k_BT}\right) + \rho_3^{-1}\exp\left(-\frac{\varepsilon_3^{\rho}}{k_BT}\right), \tag{1}$$

where the first term describes the activation of current carriers ε_1^{ρ} from the Fermi level ε_F into the zone of continuous energies, and the second, low-temperature, hopping conduction through the impurity states ε_3^{ρ} with energies close to the Fermi energy ε_F. Calculations showed that in the basic semiconductor *p-TmNiSb* the Fermi level ε_F is located at a distance of $\varepsilon_1^{\rho} = 53.4$ *meV* from the ceiling of the valence band ε_V. This result coincides with the one obtained earlier [5].

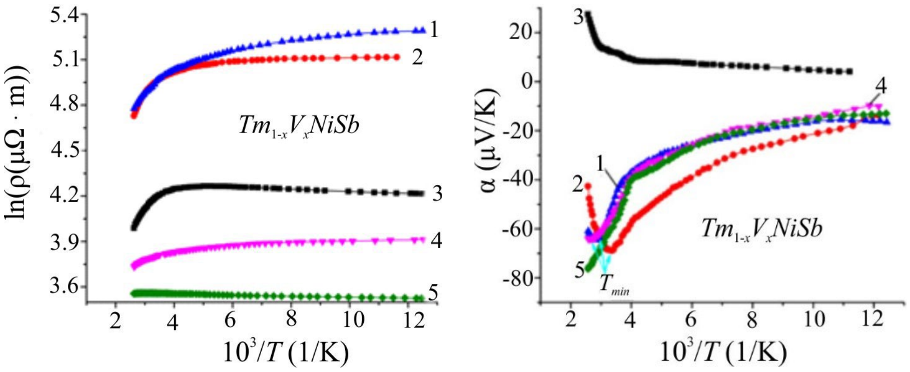

a) *b)*

*Fig. 4. Temperature dependences of resistivity $\ln(\rho(1/Tx))$ (**a**) and the Seebeck coefficient $\alpha(1/T,x)$ (b) of $Tm_{1-x}V_xNiSb$: 1 – x=0.05; 2 – x=0.03; 3 – x=0.02; 4 – x=0.08; 5 – x=0.10*

From the activation sections of the dependences of the Sebeck coefficient $\alpha(1/T)$ of $Tm_{1-x}V_xNiSb$ (Fig. 4*b*), which are described by expression (2) [12], the values of the activation energies ε_1^{α} and ε_3^{α}, were calculated, which give, respectively, the values of the modulation amplitude of continuous energy zones and small-scale fluctuations of a heavily doped and compensated semiconductor [10]:

$$\alpha = \frac{k_B}{e}\left(\frac{\varepsilon_i^{\alpha}}{k_BT} - \gamma + 1\right), \tag{2}$$

where γ is a parameter that depends on the nature of scattering mechanism.

Doping *p-TmNiSb* with the lowest in the experiment concentration of *V* atoms by substituting *Tm* atoms in the 4*a* position at concentrations $x = 0 - 0.02$ is accompanied by a decrease in the value of the electrical resistivity $\rho(x, T)$ for all investigated temperatures, for instance, at $T = 80$ K from

$\rho_{x=0}$ = 91.1 μOhm·m to $\rho_{x=0.02}$ = 67.7 μOhm·m. In doing so, the values of the Seebeck coefficient α(*x*, *T*) at these concentrations and the studied temperatures remain positive, pointing to the location of the Fermi level ε_F in the bandgap ε_g near the valence band ε_V (Figs. 5, 6).

A decrease in the values of the electrical resistivity ρ(*x, T*) of $Tm_{1-x}V_xNiSb$ at concentrations *x* = 0 - 0.02 in the hole-type semiconductor is possible only in the case of increasing the concentration of free holes during the ionization of acceptors. Incidentally, we recall that in this area of concentrations there was an increase in the values of the unit cell period *a*(*x*) (Fig. 3), and this is possible only if the *V* atoms occupy the 4*c* position of the *Ni* atoms. Since the *V* ($3d^34s^2$) atom has fewer *d*-electrons than the *Ni* ($3d^84s^2$) atom, this substitution generates structural defects of an acceptor nature, and corresponding acceptor states appear in the bandgap. It is their contribution that is decisive in reducing the values of the resistivity ρ(*x, T*) of $Tm_{1-x}V_xNiSb$ at *x* = 0 - 0.02.

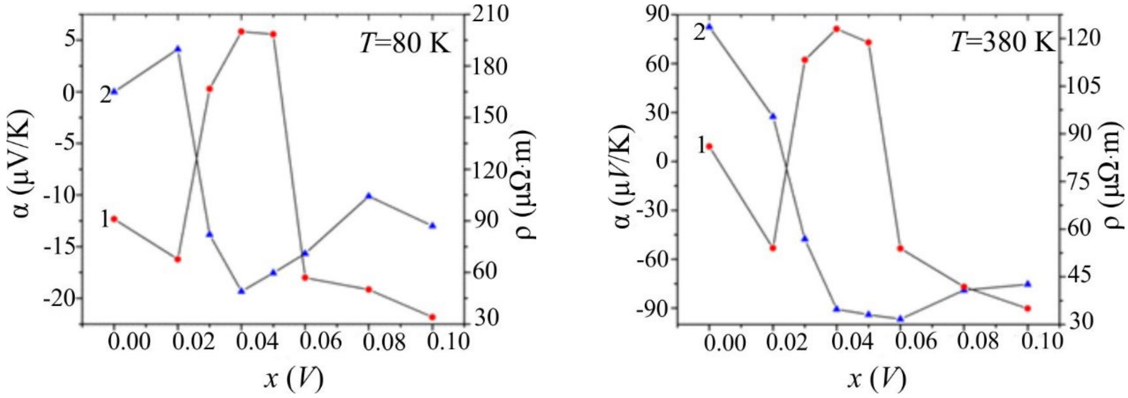

Fig. 5. Change in the values of the electrical resistivity ρ(x,T) and the Seebeck coefficient α(x,T) of $Tm_{1-x}V_xNiSb$ at different temperatures

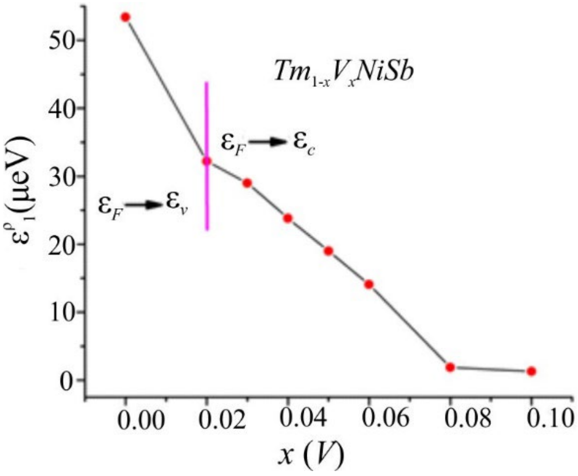

Fig. 6. Change in the values of activation energy $\varepsilon_1^{\rho}(x)$ of $Tm_{1-x}V_xNiSb$

Analysis of the behaviour of the Fermi level ε_F in the area of concentrations *x* = 0 - 0.02 also indicates an increase in the concentration of acceptor states in $Tm_{1-x}V_xNiSb$ (Fig. 6). If in *p-TmNiSb* the Fermi level ε_F is located at a distance of ε_F = 53.4 meV from the ceiling of the valence band ε_V, then in $Tm_{0.98}V_{0.02}NiSb$ it has approached the valence band at a distance of ε_F = 32.2 meV. And this is possible in a *p*-type semiconductor only if the concentration of acceptor states increases. At higher concentrations of *V* atoms in the region 0.02 < *x* ≤ 0.04, the values of the resistivity ρ(*x, T*) $Tm_{1-x}V_xNiSb$ increase, for example, at $T = 80$ K from $\rho_{x=0.02} = 67.7$ μΩ·m to $\rho_{x=0.04} = 200.3$ μΩ·m. At a concentration of $x \approx 0.03$, the sign of the Seebeck coefficient α(x, T) changes from positive to negative, and electrons become the majority carriers. An increase in the values of electrical resistivity ρ(x, T) in the concentration range $0.02 < x \leq 0.04$ and a change in the sign of the Seebeck coefficient α(x, T) is evidence of the appearance in the semiconductor of a powerful source of free electrons, which are carried away by acceptors, which leads to a decrease in the concentration of holes.

In the semiconductor $Tm_{0.97}V_{0.03}NiSb$, the concentrations of ionized acceptor and donor states are close, but there are more donors. At higher concentrations, electrons become the majority carriers in $Tm_{1-x}V_xNiSb$. We associate the decrease in the values of electrical resistivity ρ(x, T) and the negative values of the Seebeck coefficient $\alpha(x, T)$ of $Tm_{1-x}V_xNiSb$ at concentrations $0.04 < x$ (Fig. 5) with an increase in the concentration of free electrons. The results of structural studies allow us to establish their origin. Thus, at concentrations of $0.03 < x$, there is a decrease in the unit cell period $\alpha(x)$ of $Tm_{1-x}V_xNiSb$ (Fig. 3). And this is possible only when Tm atoms (($r_{Tm} = 0.174$ nмм) nm) are replaced by V atoms ($r_V = 0.134$ nm) in crystallographic position 4α. Given that V atoms $3d^34s^2$) have more d-electrons than Tm atoms ($5d^06s^2$), defects of donor nature appear in $Tm_{1-x}V_xNiSb$, and corresponding donor states appear in the bandgap.

In addition, an increase in the concentration of donor states is accompanied by a drift of the Fermi level ε_F to the conduction band ε_C almost linearly (Fig. 6). Thus, if in $Tm_{0.96}V_{0.04}NiSb$ the Fermi level ε_F lay at a distance of $\varepsilon_F = 24.1$ meV from the bottom of the conduction band ε_C,, then in the semiconductors $Tm_{0.94}V_{0.06}NiSb$ and $Tm_{0.90}V_{0.10}NiSb$ the depth of the Fermi level ε_F is $\varepsilon_F = 14.1$ meV and $\varepsilon_F = 1.3$ meV, respectively.

In this context, it seems logical to ask why the Fermi level ε_F at colossal concentrations of V atoms generating donors remains in the band gap ε_g of $Tm_{1-x}V_xNiSb$ and does not enter the conduction band ε_C? After all, donor states are generated in $Tm_{1-x}V_xNiSb$ at these concentrations. In other words, what structural changes of $Tm_{1-x}V_xNiSb$ could cause such a significant impact on the electronic system of the semiconductor that the dielectric-metal conduction transition, which is the Anderson transition [12], did not occur?

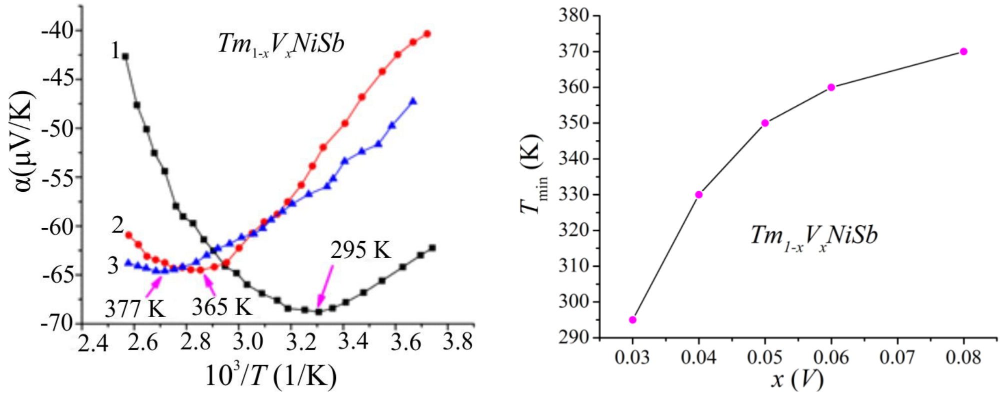

*Fig. 7. Change in the values of the Seebeck coefficient α(1/T,x): 1 – x=0.03; 2 – x=0.05; 3 – x=0.08 (**a**) and T_{min} on the dependence α((1/T,x) (b) $Tm_{1-x}V_xNiSb$*

The answer to this question is partially provided by the analysis of the behaviour of the temperature dependences of the Seebeck coefficient α(1/T, x) of $Tm_{1-x}V_xNiSb$ (Fig 4b and 7). Fig. 7a in an enlarged format shows fragments of the temperature dependences of the Seebeck coefficient α(1/T) of $Tm_{1-x}V_xNiSb$ (Fig, 4b) for three concentrations of V atoms: $x = 0.03$, $x = 0.05$ and $x = 0.08$. We recall that at all investigated temperatures the sign of the Seebeck coefficient α(1/T, x) remained positive at concentrations of $x = 0 - 0.02$. In the semiconductor $Tm_{0.97}V_{0.03}NiSb$ the sign of the Seebeck coefficient $\alpha(1/T, x)$ is already negative but the behaviour of the dependence $\alpha(1/T, x)$ turned out to be non-monotonic (Fig. 7*a*). We can see that at a temperature of $T_{\min} \approx 295$ K, the dependence passes through a minimum, and as the temperature increases, the values of the Seebeck coefficient decrease rapidly, and the dependence itself changes with a tendency to a possible change of sign at higher temperatures, which we did not reach in the experiment. This minimum on the dependence $\alpha(1/T, x)$ of $Tm_{0.97}V_{0.03}NiSb$ at the temperature $T_{\min} \approx 295$ K indicates the presence of acceptor states of unknown origin in the semiconductor of the electronic conductivity type, the contribution of which to the conductivity increases with a rise in temperature. The temperature dependences of the Seebeck coefficient $\alpha(1/T, x)$ of semiconductors $Tm_{0.95}V_{0.05}NiSb$ and $Tm_{0.92}V_{0.08}NiSb$ also have minima at temperatures $T_{\min} \approx 365$ K and $T_{\min} \approx 377$ K, respectively. However, at the highest *V* concentration, there is no such minimum on the temperature dependence $\alpha(1/T, x)$ of the $Tm_{0.90}V_{0.10}NiSb$ semiconductor, hence the influence of acceptor states on the behaviour of the Seebeck coefficient at the studied temperatures was not revealed. Fig. 7*b* shows the experimentally determined dependence of temperature minima ($T_{\min}$) on the dependence of the Seebeck coefficient $\alpha(1/T, x)$ on the concentration of impurity *V* atoms in $Tm_{1-x}V_xNiSb$. We can see that the higher the concentration of *V* atoms, the higher the temperature at which a minimum appears on the dependence of the Seebeck coefficient $\alpha(1/T, x)$.

Since the Seebeck coefficient by its nature is sensitive to a change in the ratio of current carriers of different signs, the change in the behavior of the Seebeck coefficient $\alpha(1/T, x)$ in the semiconductor now of the electronic conductivity type $Tm_{1-x}V_xNiSb$, $0.03 < x$, is manifestation of the influence of acceptor states of unknown nature on its electronic structure.

It turns out that the acceptor states that appear in $Tm_{1-x}V_xNiSb$ at high temperatures have a different depth and origin than the acceptor states caused by vacancies in the 4*a* position of *Tm* atoms. We can assume, as in the case of the related solid solution $Lu_{1-x}V_xNiSb$ [6], that in $Tm_{1-x}V_xNiSb$, the *V* ($3d^34s^2$) atoms simultaneously in different proportions occupy both position 4*a* (vacancies and replace *Tm* atoms), and replace in position 4*c* the atoms of *Ni* ($3d^84s^2$), generating structural defects of donor and acceptor nature and the respective energy states. At the same time, a question may arise regarding the correlation of such a conclusion with a change in the unit cell period which should increase when the *Ni* atoms ($r_{Ni} = 0.125$ nm) are replaced by *V* ($r_V = 0.134$ nm). We analyze the range of concentrations by which both the unit cell period *a* (*x*) of $Tm_{1-x}V_xNiSb$ (Fig. 3), and the value of electrical resistivity $\rho(x, T)$ decrease (Fig 5).

In this context, it is important to understand that the unit cell period $\alpha(x)$ of $Tm_{1-x}V_xNiSb$ is an integral parameter, reflecting changes in the semiconductor structure. Thus, the atomic radius of *Tm* is much larger than the atomic radius of *V*, and their ratio is $r_{Tm}/r_V = 1.30$. In turn, the atomic radius of *V* is slightly larger than the atomic radius of *Ni,* and their ratio is equal to $r_V/r_{Ni} = 1.07$. Therefore, the contribution to the change in the unit cell period $\alpha(x)$ of $Tm_{1-x}V_xNiSb$ from structural changes in position 4*a* of *Tm* atoms is decisive. Even under the hypothetical condition of the same distribution of impurity *V* atoms in positions 4*a* and 4*c* the values of the unit cell period *a* (*x*) of $Tm_{1-x}V_xNiSb$ will decrease.

The final establishment of the nature of the detected anomalies in the behavior of the Seebeck coefficient $\alpha(1/T, x)$ of $Tm_{1-x}V_xNiSb$ requires additional research, in particular, modeling the behavior of the Fermi level ε_F under different variants of the spatial arrangement of atoms in the array of the basic semiconductor *p-TmNiSb* and their comparison with experimental the results of this work. This will make it possible to establish the peculiarities of the crystal and electronic structure of *p-TmNiSb*, since they determine the way impurity atoms enter the array of the semiconductor, which determines the formation of structural defects of various nature and the appearance of the corresponding energy states in the bandgap ε_g. However, this is the task of another study.

Conclusions

According to the results of a comprehensive study of the structural, kinetic, and energy properties of the $Tm_{1-x}V_xNiSb$ semiconductor solid solution obtained by introducing *V* atoms into the *p-TmNiSb* structure by substituting *Tm* atoms in the crystallographic position 4*a*, a complex nature of structural changes was revealed. It is shown that *V* atoms can simultaneously occupy different crystallographic positions in different ratios, generating structural defects of acceptor and donor nature. This gives rise to the corresponding acceptor and donor states in the bandgap ε_g of $Tm_{1-x}V_xNiSb$. The mechanism of formation of two types of acceptor states with different depth of occurrence in $Tm_{1-x}V_xNiSb$: shallow acceptor states generated by vacancies in the structure of the half-Heusler phase *TmNiSb* and deep acceptor states formed by defects when *Ni* atoms are replaced by *V* in the 4*c* position. The ratio of the concentrations of generated defects determines the position of the Fermi level ε_F and the conduction mechanisms. The investigated $Tm_{1-x}V_xNiSb$ solid solution is a promising thermoelectric material.

References

1. Romaka V. A., Stadnyk Yu. V., Krayovskyy V. Ya., Romaka L. P., Guk O. P., Romaka V. V., Mykyuchuk M. M., Horyn A. M. (2020). *Novitni termochutlyvi materialy ta peretvoriuvachi temperatury* [*New thermosensitive materials and temperature converters*]. Lviv, Lvivska Polytechnika [in Ukrainian].
2. Anatychuk L. I. (1979). *Termoelementy i termoelectricheskiie ustroistva. Spravochnik.* [*Thermoelements and thermoelectric devices*. *Reference book*]. Kyiv: Naukova dumka [in Russian].
3. Hartjes K., Jeitschko W. (1995). Crystal structure and magnetic properties of the lanthanoid nickel antimonides *LnNiSb* (*Ln = La–Nd*, *Sm*, *Gd–Tm*, *Lu*). *Journal of Alloys and Compounds*, 226, 81 – 86. DOI: https://doi.org/10.1016/0925-8388(95)01573-6.
4. Karla I., Pierre J., Skolozdra R. V. (1998). Physical properties and giant magnetoresistance in *RNiSb* compounds. *Journal of Alloys and Compounds*, 265, 42 - 48. DOI: https://doi.org/10.1016/S0925-8388(97)00419-2.
5. Romaka V.V., Romaka L., Horyn A., Stadnyk Yu. (2021). Experimental and theoretical investigation of the *Y-Ni-Sb* and *Tm-Ni-Sb* systems. *Journal of Alloys and Compounds*, 855, 157334 – 12. DOI: https://doi.org/10.1016/j.jallcom.2020.157334.
6. Romaka V. V., Romaka V. A., Stadnyk Yu. V., Romaka L. P., Plevachuk Y. O., Pashkevich V. Z., Haraniuk P. I. Horyn A. (2023). Features of the generation of the energy states in the semiconductor $Lu_{1-x}V_xNiSb$. *Ukr. J. Phys*., 68 (№ 4), 274 – 283. DOI: https://doi.org/10.15407/ujpe68.4.274.
7. Romaka V. A., Stadnyk Yu., Romaka L., Horyn A., Pashkevich V., Nychyporuk H., Garanyuk P. (2022). Investigation of Thermoelectric Material Based on $Lu_{1-x}Zr_xNiSb$ Solid Solution. I. Experimental Results. *J. Phys. and Chem. Sol. State*, 23, 235–241. DOI: 10.15330/pcss.23.2.235-241.
8. Romaka V. V., Romaka V. A., Stadnyk Yu. V., Romaka L. P., Demchenko P. Yu., Pashkevich V. Z., Horyn A. M. (2022). Features of mechanisms of electrical conductivity in semiconductive solid solution $Lu_{1-x}Sc_xNiSb$. *Ukr. J. Phys*., 67 (№ 5), 370–379. DOI: https://doi.org/10.15407/ujpe67.5.370.
9. Roisnel T., Rodriguez-Carvajal J. (2001). WinPLOTR: a windows tool for powder diffraction patterns analysis. *Mater. Sci. Forum*, Proc. EPDIC7 378 – 381, 118 – 123. DOI: https://doi.org/10.4028/www.scientific.net/MSF.378-381.118.

10. Shklovskii B. I. and Efros A. L. (1984). *Electronic properties of doped semiconductors* NY: Springer; (1979) Moscow: Nauka. DOI: https://doi.org/10.1002/crat.19720070420.
11. Babak V. P., Babak S. V., Myslovych M. V., Zaporozhets A. O., Zvaritch V. M. (2020). Technical provision of diagnostic systems. *Studies in Systems, Decision and Control*, 281, 91 – 133. DOI: https://doi.org/10.1007/978-3-030-44443-3_4.
12. Mott N. F., Davis E. A. (1979). *Electron processes in non-crystalline materials.* Oxford: Clarendon Press. DOI: 10.1007/978-3-662-02403-4.

Submitted: 26.01.2023

Ромака В. А., *док. тех. наук,*
канд. фіз.-мат. наук, професор[1]
Стадник Ю. В, *канд. хім. наук*[2]
Ромака Л. П., *канд. хім. наук*[2]
Демченко П. Ю.[2]**,**
Горинь А. М., *канд. хім. наук*[2]
Луковський Т. І.[1]

[1]Національний університет "Львівська політехніка", вул. С. Бандери, 12,
Львів, 79013, Україна; *e-mail: vromaka@polynet.lviv.ua*
[2]Львівський національний університет ім. І. Франка, вул. Кирила і Мефодія, 6,
Львів, 79005, Україна; *e-mail: lyubov.romaka@lnu.edu.ua*

ЕКСПЕРИМЕНТАЛЬНІ ДОСЛІДЖЕННЯ ВЛАСТИВОСТЕЙ НОВОГО ТЕРМОЕЛЕКТРИЧНОГО МАТЕРІАЛУ $Tm_{1-x}V_xNiSb$

Досліджено структурні, кінетичні та енергетичні властивості термоелектричного матеріалу $Tm_{1-x}V_xNiSb$ у діапазонах: $T = 80 – 400$ К, $x = 0 – 0.10$. Показано, що атоми V можуть одночасно у різних співвідношеннях займати різні кристалографічні позиції, генеруючи дефекти акцепторної та донорної природи. Це породжує у забороненій зоні ε_g $Tm_{1-x}V_xNiSb$ відповідні акцепторні та донорні стани. Встановлено механізм формування у $Tm_{1-x}V_xNiSb$ двох сортів акцепторних станів з різною глибиною залягання: дрібні акцептори, породжена вакансіями у структурі фази пів-Гейслера TmNiSb, та глибокі акцептори, утворені дефектами при заміщенні у позиції 4c атомів Ni на V. Співвідношення концентрацій генерованих дефектів визначає положення рівня Фермі ε_F та механізми провідності. Досліджений твердий розчин $Tm_{1-x}V_xNiSb$ є перспективним термоелектричним матеріалом. Бібл. 12, рис. 7.

Ключові слова: *електронна структура, електроопір, коефіцієнт термоЕРС.*

References

1. Romaka V. A., Stadnyk Yu. V., Krayovskyy V. Ya., Romaka L. P., Guk O. P., Romaka V. V., Mykyuchuk M. M., Horyn A. M. (2020). *Novitni termochutlyvi materialy ta peretvoriuvachi*

temperatury [*New thermosensitive materials and temperature converters*]. Lviv, Lvivska Polytechnika [in Ukrainian].

2. Anatychuk L. I. (1979). *Termoelementy i termoelectricheskiie ustroistva. Spravochnik.* [*Thermoelements and thermoelectric devices*. *Reference book*]. Kyiv: Naukova dumka [in Russian].
3. Hartjes K., Jeitschko W. (1995). Crystal structure and magnetic properties of the lanthanoid nickel antimonides *LnNiSb* (*Ln* = *La–Nd*, *Sm*, *Gd–Tm*, *Lu*). *Journal of Alloys and Compounds*, 226, 81 - 86. DOI: https://doi.org/10.1016/0925-8388(95)01573-6.
4. Karla I., Pierre J., Skolozdra R. V. (1998). Physical properties and giant magnetoresistance in *RNiSb* compounds. *Journal of Alloys and Compounds*, 265, 42 - 48. DOI: https://doi.org/10.1016/S0925-8388(97)00419-2.
5. Romaka V.V., Romaka L., Horyn A., Stadnyk Yu. (2021). Experimental and theoretical investigation of the *Y-Ni-Sb* and *Tm-Ni-Sb* systems. *Journal of Alloys and Compounds*, 855, 157334 – 12. DOI: https://doi.org/10.1016/j.jallcom.2020.157334.
6. Romaka V. V., Romaka V. A., Stadnyk Yu. V., Romaka L. P., Plevachuk Y. O., Pashkevich V. Z., Haraniuk P. I. Horyn A. (2023). Features of the generation of the energy states in the semiconductor $Lu_{1-x}V_xNiSb$. *Ukr. J. Phys*., 68 (№ 4), 274 – 283. DOI: https://doi.org/10.15407/ujpe68.4.274.
7. Romaka V. A., Stadnyk Yu., Romaka L., Horyn A., Pashkevich V., Nychyporuk H., Garanyuk P. (2022). Investigation of Thermoelectric Material Based on $Lu_{1-x}Zr_xNiSb$ Solid Solution. I. Experimental Results. *J. Phys. and Chem. Sol. State*, 23, 235–241. DOI: 10.15330/pcss.23.2.235-241.
8. Romaka V. V., Romaka V. A., Stadnyk Yu. V., Romaka L. P., Demchenko P. Yu., Pashkevich V. Z., Horyn A. M. (2022). Features of mechanisms of electrical conductivity in semiconductive solid solution $Lu_{1-x}Sc_xNiSb$. *Ukr. J. Phys*., 67 (№ 5), 370 – 379. DOI: https://doi.org/10.15407/ujpe67.5.370.
9. Roisnel T., Rodriguez-Carvajal J. (2001). WinPLOTR: a windows tool for powder diffraction patterns analysis. *Mater. Sci. Forum*, Proc. EPDIC7 378 - 381, 118 – 123. DOI: https://doi.org/10.4028/www.scientific.net/MSF.378-381.118.
10. Shklovskii B. I. and Efros A. L. (1984). *Electronic properties of doped semiconductors* NY: Springer; (1979) Moscow: Nauka. DOI: https://doi.org/10.1002/crat.19720070420.
11. Babak V. P., Babak S. V., Myslovych M. V., Zaporozhets A. O., Zvaritch V. M. (2020). Technical provision of diagnostic systems. *Studies in Systems, Decision and Control*, 281, 91 – 133. DOI: https://doi.org/10.1007/978-3-030-44443-3_4.
12. Mott N. F., Davis E. A. (1979). *Electron processes in non-crystalline materials.* Oxford: Clarendon Press. DOI: 10.1007/978-3-662-02403-4.

Submitted: 26.01.2023